Optimized regional and interannual variability of lightning in a global chemical transport model constrained by LIS/OTD satellite data

Optimized regional and interannual variability of lightning in a global chemical transport model constrained by LIS/OTD satellite data

Murray, Lee T.[1], *Daniel J. Jacob* [1], *Jennifer A. Logan* [1], *Rynda C. Hudman* [1,*], *William J. Koshak* [2]

1. Harvard School of Engineering and Applied Sciences, 29 Oxford St, Cambridge, MA, 02138, USA

2. Earth Science Office, ZP11, NASA Marshall Space Flight Center, Huntsville, AL, 35805, USA

* Now at US EPA

Submitted to *J. Geophys. Res.*

Abstract

Nitrogen oxides ($NO_x \equiv NO + NO_2$) produced by lightning make a major contribution to the global production of tropospheric ozone and OH. Lightning distributions inferred from standard convective parameterizations in global chemical transport models (CTMs) fail to reproduce observations from the Lightning Imaging Sensor (LIS) and the Optical Transient Detector (OTD) satellite instruments. We present an optimal regional scaling algorithm for CTMs to fit the lightning NO_x source to the satellite lightning data in a way that preserves the coupling to deep convective transport. We show that monthly scaling using ~35 global regions significantly improves the tropical ozone simulation in the GEOS-Chem CTM as compared to a simulation unconstrained by the satellite data, and performs equally well to a simulation with local scaling. The coarse regional scaling preserves sufficient statistics in the satellite data to constrain the interannual variability (IAV) of lightning. After processing the LIS data to remove its diurnal sampling bias, we construct a monthly time series of lightning flash rates for 1998-2010 and 35ºS-35ºN. We find a correlation of IAV in tropical lightning with El Niño but not with the solar cycle or the quasi-biennial oscillation. The resulting global lightning NO_x source in GEOS-Chem is 6.0 ± 0.5 Tg N a^{-1}, compared to 5.5 ± 0.8 Tg N a^{-1} for the biomass burning source. Lightning NO_x could have a large influence on the IAV of tropospheric ozone because it is released in the upper troposphere where ozone production is most efficient.

1. Introduction

The extreme heat in a lightning flash channel converts atmospheric N_2 and O_2 to nitrogen oxide radicals ($NO_x \equiv NO + NO_2$) that drive the formation of tropospheric ozone and influence OH, the principal tropospheric oxidant [*Chameides et al.*, 1977; *Logan et al.*, 1981; *Labrador et al.*, 2004]. The global source of NO_x from lightning is smaller than the source from combustion, but its impact on ozone is disproportionately large because it is mainly released in the upper troposphere where the lifetimes of NO_x and ozone are long [*Pickering et al.*, 1990; *Hauglustaine et al.*, 1994]. Lightning is the least understood of atmospheric NO_x sources, with global estimates in the range 1-20 Tg N a^{-1} [*Schumann and Huntrieser*, 2007]. Parameterizations used in global chemical transport models (CTMs) show little skill in reproducing observed lightning distributions [*Tost et al.*, 2007; *Sauvage et al.*, 2007b]. Here we develop a method for using satellite observations to constrain the lightning source in global CTMs in a way that preserves the coupling to convective transport and allows investigation of interannual variability of lightning influence. In a companion paper [*Murray et al.*, *in prep.*], we apply this method to examine the role of lightning in driving the interannual variability of ozone and OH in the tropical troposphere.

Quantifying the source of lightning NO_x from first principles is hindered by uncertainties in the physics of lightning formation. Enormous local electric potentials of up to ±100 MV with respect to the ground develop inside thunderstorms and are subsequently dissipated in part by lightning [*Marshall and Stolzenburg*, 2001]. The mechanisms that lead to the development of these differences in potential are still being debated [*Rakov and Uman*, 2003, and references therein]. The cloud scales involved in lightning generation are much smaller than the typical grid size in global models, requiring sub-grid parameterizations. Parameterization of lightning must be consistent with the model convective transport, because mixing of lightning NO_x with boundary layer gases brought up by convection greatly enhances the resulting ozone production in the upper troposphere [*Pickering et al.*, 1993; *Jaeglé et al.*, 2001]. Simply prescribing lightning in the CTM on the basis of observational data would not guarantee such consistency.

A number of lightning flash rate parameterizations for global and regional models have been developed, all based on proxies of deep convection [*Price and Rind*, 1992; 1993; 1994; *Price et al.*, 1997; *Allen et al.*, 2000; *Grewe et al.*, 2001; *Meijer et al.*, 2001; *Allen and Pickering*, 2002; *Petersen et al.*, 2005; *Jacobson and Streets*, 2009]. *Tost et al.* [2007] examined four commonly used lightning schemes within a suite of convective parameterizations, and found that all combinations failed to reproduce the observed global lightning distributions from the combined climatologies of the Optical Transient Detector (OTD) and the Lightning Imaging Sensor (LIS) satellite instruments [*Christian et al.*, 2003].

Here we explore optimal ways to use the LIS/OTD satellite observations to improve the representation of lightning in CTMs, using as testbed the GEOS-Chem CTM [*Bey et al.*, 2001]. Climatological LIS/OTD data have been used previously in CTMs to apply correction factors on various scales to the lightning flash rate parameterizations. Local correction factors [*Sauvage et al.*, 2007b; *Allen et al.*, 2010] provide maximum fidelity to the spatial and seasonal distribution of lightning observations but are least consistent with the distribution of model convective transport and also suffer from relatively few observations per grid cell. Correction factors applied to large regions [*Stajner et al.*, 2008; *Jourdain et al.*, 2010] have less fidelity to observations but are more statistically robust and are more consistent with the model convective transport. All studies so far have used lightning observations averaged over a number of years in order to have adequate statistics but interannual variability is then not resolved. Here we develop an optimal algorithm for selecting coherent lightning regions over which to apply correction factors, and we use an improved LIS/OTD data set to examine the sensitivity of CTM results to the scales over which the correction factors are applied. We show that adequate fidelity to lightning observations can be achieved with regions sufficiently coarse to constrain the interannual variability in lightning and investigate the resulting impact on atmospheric chemistry.

2. Satellite lightning observations

We use satellite observations from the OTD for May 1995 to December 2000, and its successor the LIS for December 1997 to present. The two instruments detect total optical pulses from cloud-to-ground (CG) and intra-cloud (IC) lightning flashes during both day and night, with a clustering algorithm used to lump the optical pulse events into individual flashes [*Christian et al.*, 1989; *Boccippio et al.*, 2000; 2002; *Mach et al.*, 2007]. OTD flew on the Microlab I satellite with near-global coverage (75°S-75°N), and detection efficiencies (DEs) of 35-55% relative to regional ground-based detection networks. LIS is a component of the NASA Tropical Rain Measuring Mission (TRMM), with a narrower latitudinal range of 35°S-35°N, and higher DEs of about 70-90% [*Koshak et al.*, 2000; *Boccippio et al.*, 2002; *Christian et al.*, 2003; *Mach et al.*, 2007].

In this study, we use two products available from the NASA Global Hydrology and Climate Center (GHCC; http://thunder.msfc.nasa.gov/): (1) the High Resolution Monthly Climatology (HRMC) gridded product version 2.2, and (2) the LIS Science Data version 4.1. The HRMC gridded product consists of long-term monthly mean flash densities (km^{-2} d^{-1}) from OTD and LIS averaged over 1995-2005, inter-calibrated and with corrections applied for their respective DEs. This product is prepared by GHCC at a resolution of 0.5° × 0.5°, using spatial smoothing of 2.5°. It improves over the earlier LIS/OTD gridded products from GHCC by (1) using more years of data, (2) providing monthly temporal resolution instead of seasonal, and (3) providing finer spatial scale. The LIS Science Data product available for December 1997 to present contains the individual orbital data for lightning flashes on a 0.5°x0.5° grid. This product has been filtered for

noise and quality assurance, and corrected for DE. We omit observations with bad data or warning flags.

3. GEOS-Chem chemical transport model

The GEOS-Chem global 3-D CTM (version 9.01.01; http://www.geos-chem.org) simulates tropospheric ozone-NO_x-CO-hydrocarbon-aerosol chemistry with transport driven by assimilated meteorological fields from the Goddard Earth Observing System (GEOS) of the NASA Global Modeling and Assimilation Office (GMAO). Here we use archived GEOS-4 fields for 2003-2005, with 2003 used for model initialization. The meteorological data are 6 h means (3 h for surface fields and mixing depths) and have horizontal resolution of 1º latitude by 1.25º longitude with 55 layers in the vertical. We degrade the horizontal resolution to 2º by 2.5º for input to GEOS-Chem. Convective transport in GEOS-Chem mimics that in the parent GEOS general circulation model (GCM) [*Hack*, 1994; *Zhang and McFarlane*, 1995]. It uses 6 h GEOS-4 data for updraft, downdraft, and entrainment mass fluxes archived separately for deep and shallow convection [*Wu et al.*, 2007]. For this work we have updated the GEOS-Chem chemistry module in the stratosphere by archiving monthly mean production and loss frequencies of species from the NASA Global Modeling Initiative (GMI) Combo CTM Aura4 simulations using GEOS-4 meteorology [*Duncan et al.*, 2007; *Considine et al.*, 2008; *Allen et al.*, 2010].

Table 1 summarizes the global NO_x sources in GEOS-Chem for 2004-2005. The lightning source is described in Section 4. Anthropogenic sources are from the Emission Database for Global Atmospheric Research (EDGAR) base inventory for 2000 [*Olivier*, 2001], overwritten with regional inventories for the United States (EPA NEI2005), Canada (CAC), Mexico (BRAVO) [*Kuhns et al.*, 2003], Europe (EMEP) [*Auvray and Bey*, 2005], and South and East Asia [*Streets et al.*, 2003; 2006], and scaled for each year as described by *Van Donkelaar et al*. [2008]. Biofuel emissions are from *Yevich and Logan* [2003]. Biomass burning emissions are from the Global Fire Emissions Database (GFED v2) [*van der Werf et al.*, 2006]. Soil NO_x emissions follow the *Yienger and Levy* [1995] parameterization as implemented by *Wang et al*. [1998].

4. Lightning source of NO_x

4.1 Unconstrained parameterization

The use of a convection-based lightning parameterization in the CTM is necessary, even if it is to be subsequently adjusted by the lightning data, because it allows the corrected lightning to still be co-located with the convective transport in the model. We refer to a parameterization that relies solely on model convection variables as “unconstrained” since it is not constrained by the satellite lightning data. The standard GEOS-Chem model uses the Cloud Top Height (CTH) parameterization of *Price and Rind* [1992;

1993; 1994], who fit observed lightning frequency to a fifth-power function of CTH over continents and extrapolated a second-power function over oceans. The CTH in each deep convective model column is determined as the altitude where the upward convective mass flux vanishes to zero. The original *Price and Rind* [1992] parameterization treated grid cells up to 500 km from shore as continental, but here we treat grid cells as continental only if they contain over 50% land, which is more in keeping with the observed land-sea contrast in the LIS/OTD HRMC product. We also evaluate two alternative flash rate parameterizations: the convective mass flux scheme (MFLUX) of *Allen et al.* [2000] used as the base parameterization for the GMI model [*Allen et al.*, 2010], and the convective precipitation (PRECON) scheme of *Allen and Pickering* [2002]. As the latter two determine cloud-to-ground (CG) but not intra-cloud (IC) flash densities, we infer total (IC+CG) flashes locally using the IC/CG ratio parameterization from *Price and Rind* [1993]. Each parameterization is adjusted by a dimensionless uniform scaling parameter β, following *Tost et al.* [2007], to bring the annual average global flash rate to that of the observed LIS/OTD HRMC product, 46 flashes s^{-1} [*Christian et al.*, 2003].

Because the maximum negative charge layer encompasses a vertical region from 0°C to -40°C [*Williams*, 1985], any grid cell with a surface temperature less than -40ºC is assumed too cold for lightning. In addition, any convective column that does not span the full temperature range of the negative charge layer is assumed to be insufficient for lightning. This shallow cloud inhibition prevents parameterized lightning in regions of persistent marine stratus clouds, e.g., off the coast of Peru and Chile.

Figure 1 compares each of the three unconstrained lightning flash rate parameterizations in GEOS-Chem with the LIS/OTD HRMC climatology. The schemes capture less than half of the variability of the observations at 2º x 2.5º monthly resolution (CTH: R = 0.66; MFLUX: R = 0.40; PRECON: R = 0.41; n = 144 longitudes x 91 latitudes x 12 months). None captures the strong maximum observed over central Africa and all have excessive lightning over Oceania. The MFLUX and PRECON parameterizations have spurious lightning over the tropical oceans, and their inability to reproduce the land-sea contrast is the primary reason for their lower correlation coefficients. Much of the CTH error comes from poor seasonality. As the CTH scheme yields the best a priori distribution of the three approaches, we choose to use it as our unconstrained physical parameterization. *Tost et al*. [2007] also found it to be the most accurate lightning distribution model and most robust within different convective model frameworks.

4.2 LIS/OTD correction factors

Previous global CTMs that use the GEOS meteorological fields have constrained their flash rate parameterizations to LIS/OTD products, including GEOS-Chem [*Sauvage et al.*, 2007b; *Stajner et al.*, 2008; *Jourdain et al.*, 2010], GMI [*Allen et al.*, 2010], and the University of Maryland CTM (*D. Allen, pers. comm.*). The constraint involves correcting

the unconstrained model flash rates over selected spatial and temporal domain D by a factor α to match the climatological LIS/OTD data:

$$\alpha = \beta \iint_D F_o(\mathbf{x},t)\,\mathrm{d}\mathbf{x}\,\mathrm{d}t \Big/ \iint_D F_p(\mathbf{x},t)\,\mathrm{d}\mathbf{x}\,\mathrm{d}t \tag{1}$$

where F_o is the observed LIS/OTD flash rate over D, F_p is the corresponding value from the unconstrained model parameterization, and β was introduced previously to scale the unconstrained global flash rate to match the 46 flashes s^{-1} of the LIS/OTD data (Section 4.1). As an example, if the model simulated constant flash rates for a world divided into two hemispheres, but observations saw twice the lightning in one hemisphere than the other, the values of α would be respectively 1.5 and 0.75. Lightning variability within each domain D is governed by the CTM lightning parameterization (depending on CTH) to ensure that lightning NO_x emissions are coupled to deep convective transport. Here we impose the temporal domain to be monthly and explore the sensitivity to the choice of spatial domain, which can be the grid resolution of the CTM (local scaling) as in *Sauvage et al*. [2007b] and *Allen et al*. [2010] or a larger region (regional scaling) as in *Stajner et al*. [2008] and *Jourdain et al*. [2010].

The choice of local or regional scaling can have significant implications. Local scaling maximizes fidelity to the location of lightning in the observations but the scaling factors can range over many orders of magnitude. As a result, the amount of lightning NO_x released per convective event may be unrealistic and the dependence on the local height of convection may be lost. Large scaling factors can make the model calculate unrealistically high daily NO_2 column peaks, especially at locations with few convective events per month in the model. Using regional scaling addresses these difficulties and reduces sampling biases, but the distribution of lightning within a region may not match that in the observations.

Here we use hierarchical clustering [*Johnson*, 1967] as an objective data-driven aggregation technique to select coherent scaling regions in a way that tries to maximize the domain size (D) while preserving the fit to the observed global lightning distribution. The principal benefit of the hierarchical technique over other clustering algorithms is that it makes no prior assumptions about how the regions are to be clustered. The algorithm initially assigns each 2º x 2.5º grid square to its own region, calculates the "distance" to all other regions, and joins the two most similar; this proceeds iteratively until eventually only one region remains. We thus obtain a hierarchical tree or "dendogram" of optimally clustered regions, and can compare in the CTM the effect of choosing different levels of the dendogram (i.e., different numbers of regions). To construct the dendogram we define the "location" for a region i by the vector $\mathbf{v}_i = (\mathbf{x},a,b)^T$ where $\mathbf{x}$ is the position of the region centroid on the sphere, a is the absolute difference between the unconstrained model and the observed monthly mean flash rates averaged over the region, and b is the

logarithm of the relative difference. All variables are standardized globally to unit variance and zero mean. We then define "distance" between two regions *i* and *j* as the norm $||\mathbf{v}_i - \mathbf{v}_j||$. This aggregates regions that are geographically close (though not necessarily contiguous) and that match the observations similarly well or poorly. Coherent regions are calculated separately for each month of the year. We impose that the first branch separate between land and ocean because the CTH parameterization is different for these two domains.

Figure 2 shows the resulting redistribution of lightning in GEOS-Chem for July, for both local scaling (2ºx2.5º) and regional scaling. **Table 2** gives the corresponding redistribution statistics. We consider two levels of regional scaling, fine and coarse, corresponding to different levels of the dendogram with an average of 137 and 37 global regions respectively. The coarse resolution is still finer than the continental scales used by *Stajner et al*. [2008] and *Jourdain et al*. [2010]. As the regions increase in size, the range of scaling factors considerably decreases. Correlation with the monthly LIS/OTD climatology ranges from R = 0.66 for the unconstrained case to R > 0.99 for the local redistribution. The high bias of tropical lightning in the unconstrained parameterization is corrected. Most of the improvement in fitting the LIS/OTD data is already achieved with the coarse regional scaling and its ~37 regions (R = 0.89). We compare below the local and regional scaling approaches in terms of their effects on the GEOS-Chem simulation of ozone.

4.3 Converting flash rates to NO_x emissions

There is large uncertainty in relating flash rates to lightning NO_x emissions [*Schumann and Huntrieser*, 2007]. Standard practice in GEOS-Chem and other global CTMs has been to adjust the global lightning NO_x source to optimize the simulation of tropospheric ozone and nitrogen oxides. The range in global CTMs is 3-7 Tg N a^{-1} [*Denman et al.*, 2007]. *Martin et al*. [2007] derived a best estimate of 6 (4-8) Tg N a^{-1} in GEOS-Chem to match satellite estimates of the column of tropospheric ozone in the tropics.

There is evidence for higher NO_x yields per flash in the extratropics than in the tropics from aircraft campaigns [*Huntrieser et al.*, 2002; 2007; 2008], satellite observations [*Martin et al.*, 2006; 2007; *Sauvage et al.*, 2007b; *Boersma et al.*, 2008] and model studies [*Hudman et al.*, 2007]. We use here a yield of 500 mol N per flash from *Hudman et al*. [2007] for all extratropical lightning north of 23°N in America and 35°N in Eurasia. This yield is consistent with several studies of lightning NO_x production over the U.S. [*DeCaria et al.*, 2005; *Cooper et al.*, 2007; *Jourdain et al.*, 2010; *Ott et al.*, 2010]. For the rest of the world, we use the constraint of 4.4 Tg N a^{-1} for that region derived by *Martin et al*. [2006; 2007], together with the LIS/OTD climatological flash rate, to infer 260 mol N per flash. This is within the range of current literature [*Schumann and Huntrieser*, 2007].

Unlike earlier versions of GEOS-Chem, we do not include a dependence of the NO_x yield on the length of the flash (which is poorly constrained) or whether the flash is CG or IC [*Wang et al.*, 1998]. The studies by *Ott et al*. [2007; 2010] suggests no difference in yield between CG and IC flashes. More recent work by *Koshak et al.* [*in review*] using the NASA Lightning Nitrogen Oxides Model (LNOM), a highly detailed process-based model of NO_x production built upon lightning properties observed by ground-based networks, finds substantially higher yields in CG than IC flashes.

The lightning NO_x emitted in the model for a given grid column and 6 h period is distributed vertically between the surface and convective cloud top height following standard profiles for marine, tropical continental, subtropical, and mid-latitude storms simulated by *Ott et al*. [2010] using a cloud-resolving model. This updates the vertical profiles from *Pickering et al*. [1998] used in previous versions of GEOS-Chem. The principal difference is that *Pickering et al*. [1998] release 10-20% of LNO_x below 2 km, as compared to 1-7% in *Ott et al.* [2010],. The newer profiles also have a lower median height of emission.

5. Implications for modeling tropospheric ozone

Figure 3 shows the impacts of the different lightning redistribution methods on the GEOS-Chem simulations of lightning NO_x emissions and zonal mean tropospheric ozone. All simulations are identical except for the lightning redistribution. The dominant effect of the redistribution is to shift lightning flashes from the tropics to the extratropics, as previously found by *Sauvage et al.* [2007b]. This decreases tropical ozone while increasing extratropical ozone by up to 4 ppbv relative to the unconstrained simulation. Inspection of seasonal differences (not shown) shows similar behavior

Figure 4 compares simulated ozone with climatological profiles from four representative tropical stations of the SHADOZ network [*Thompson et al.*, 2003a]. Also shown is a simulation without lightning NO_x, which greatly underestimates observations and illustrates the model sensitivity to the lightning source of NO_x. The model reproduces the general vertical, zonal, and seasonal patterns in the observations, except over the South Atlantic during October and over equatorial Arica in July and October, as well as in the upper troposphere (UT) in April. We find that lightning redistribution changes ozone concentrations by typically a few ppbv relative to the unconstrained simulation, the largest effect being at San Cristóbal in April (-4.7 ppbv) due to excessive wet season lightning over Amazonia in the unconstrained simulation. The differences between the redistribution techniques are typically less than 1 ppbv. These effects are sufficiently small that no method emerges as significantly better for reproducing the observations.

Satellite ozone data provide a more sensitive test. We compared the different simulations with the OMI/MLS tropospheric column of ozone (TCO) product developed by *Ziemke et al*. [2006], who subtracted coincident measurements of stratospheric ozone made by the

Microwave Limb Sounder (MLS) [*Waters et al.*, 2006] from total column ozone measurements made by the Ozone Monitoring Instrument (OMI) [*Levelt et al.*, 2006], both on the Aura satellite. We determined model TCO using hourly ozone profiles and the local lapse rate tropopause, and averaged over each month. **Figure 5** compares the simulation with local redistribution to the seasonal mean observations. The model is biased low by a few DU over most of the tropics. It reproduces well the observed spatial and seasonal patterns. **Figure 6** shows the Pearson correlation coefficient for model versus observed monthly mean TCO values on the 2ºx2.5º grid for 23ºS-23ºN and for October 2004 to December 2005. Overall the model performs well, with R in the range 0.84-0.96. Lightning redistribution improves the simulation of ozone variability for almost every month. The improvements are statistically significant. Comparison of the three different redistributions shows slightly better results for the local scaling but the differences are not statistically significant.

There is a well-known zonal "wave one" pattern in tropical TCO [e.g., *Fishman et al.*, 1990; 1991; *Shiotani*, 1992; *Thompson and Hudson*, 1999; *Thompson et al.*, 2000; 2003b; *Sauvage et al.*, 2006]. We illustrate this pattern in **Figure 7** with Hovmöller plots for TCO in the latitude bands 0-23ºS and 0-23ºN as a function of longitude and time. In the southern tropics, the model reproduces the wave one pattern with a maximum over the South Atlantic and Africa (60ºW to 40ºE), peaking in September to November (SON), and a minimum over the Pacific (140-180ºE). The maximum is driven by persistent radiative subsidence over the South Atlantic anticyclone drawing in NO_x (including from lightning) and other precursors lofted by deep convection over the continents [*Krishnamurti et al.*, 1993; *Chatfield et al.*, 1996; *Jacob et al.*, 1996; *Martin et al.*, 2002; *Sauvage et al.*, 2007a]. The unconstrained model has a relatively low correlation with observations over the South Atlantic and adjacent land masses, mainly because of underestimate of the SON seasonal maximum and a 2-month early shift in the timing of the maximum. The lightning redistributions all greatly improve the correlation with observations in that region by delaying the maximum by 1 month; there is no significant difference between the different redistributions. In the northern tropics, lightning redistribution has little effect except for a large improvement over the western North Atlantic, and a modest improvement over Africa where the model shows low skill in reproducing ozone variability.

6. Interannual variability of lightning flash rates

We have shown above that the local and regional approaches for lightning redistribution using the LIS/OTD data are statistically indistinguishable in their ability to simulate tropospheric ozone, although the local redistribution may be marginally better. All improve model ozone over the unconstrained lightning simulation. An important advantage of the coarse regional over the finer redistributions is that it provides better observational statistics with which to constrain interannual variability (IAV) in flash rates and its effects on the IAV of tropical tropospheric ozone and OH, a subject of

considerable interest in the literature [*Ziemke and Chandra*, 1999; *Prinn et al.*, 2005; *Grewe*, 2007; *Duncan and Logan*, 2008; *Montzka et al.*, 2011; *Murray et al*., *in prep*.].

Here we constrain the IAV of tropical lightning using the coarse regional redistribution applied to LIS orbital data for 1998-present (Section 2). LIS is in inclined orbit and sweeps between 35ºS and 35ºN about 15 times a day. Care must be taken to correct for the interannually varying diurnal schedule of the orbit tracks as the lightning frequency varies greatly with time of day. This is illustrated in **Figure 8** with the diurnal distribution of LIS sampling for October 2002 and 2003 at 35ºN and the Equator, together with the global mean diurnal distribution of lightning observed from OTD in 1995-2000 in sun-asynchronous near-polar orbit [*Schumann and Huntrieser*, 2007]. Lightning activity is minimum at 9-10 local time (LT) and maximum at 15-16 LT. LIS observations sample this distribution very differently in October of 2002 and 2003. There is greater diurnal bias in observations at 35º than at the Equator, but observations the Equator are ten times less frequent.

The bottom panels of **Figure 8** show the diurnal sampling bias of LIS for October 2003 as measured by the relative departure from uniform daily sampling. The diurnal sampling increases from about 30% at the Equator to 60% at 35º latitude, varying little with longitude. The time required for LIS to sample all hours of day at least once ranges from about 30 days at the equator to about 98 days in the subtropics, making a local redistribution inappropriate to constrain flash rates for a specific month and year. However, the bottom panels of **Figure 8** show that regional distribution greatly reduces this diurnal bias through the merging of areas at different latitudes. This, combined with the much greater number of observations per coarse region (Table 2) allows an effective correction of the diurnal sampling bias.

We represent IAV in the global distribution of lightning in GEOS-Chem for the LIS observation domain (35ºS-35ºN) by first applying the local climatological scaling described in Section 4, and then applying the coarse regional scaling using the LIS data for individual years (1998-2010). The flash rates from the LIS Science Data 4.1 product were aggregated into 24 hourly bins (local time) for each region, month, and year. They were then adjusted with the hourly LIS detection efficiencies from *Boccipio et al*. [2002], and averaged to derive monthly regional flash rates for scaling the climatological values. In the event any hour was not observed in that region and month, the monthly mean for 1998-2010 was used. Poleward of 35º where there are no LIS data we use the LIS/OTD climatology (effectively OTD) with local redistribution and no IAV constraint; 25% of global lightning flashes are poleward of 35º and any simulated IAV there is driven by model meteorology.

Figure 9 shows the resulting flash rate time series in the tropics (23ºS-23ºN) for the 1998-2010 period. Mean lightning activity increased slowly from 1998 until early 2002 and then leveled off. Also shown are climatological indices for the solar flux and for the

El Niño-Southern Oscillation (ENSO). We correlated the 12-month running means of tropical flash rates with those of the two indices and find little correlation with the solar flux (R = -0.21) but strong correlation with the Niño Region 3.4 index (R=0.79). This suggests that ENSO plays an important role in driving IAV in tropical lightning activity. We find no correlation of lightning with the stratospheric Quasi-Biennial Oscillation (not shown), which has been previously linked to tropical deep convection [*Collimore et al.*, 1998; 2003].

The positive correlation of lightning with ENSO is consistent with previous studies for Indonesia and Southeast Asia [*Hamid et al.*, 2001; *Yoshida et al.*, 2007; *Logan et al.*, 2008] and the southeastern United States [*Goodman et al.*, 2000]. *Hamid et al*. [2001] noted that lightning frequencies in the tropics are very sensitive to small increases in surface air temperature [*Williams*, 1992] and that the surface temperature over the tropical land generally increases during El Niño events [*Hansen and Lebedeff*, 1987]. *Hamid et al.* [2001] attribute the increase in lightning activity over Indonesia to higher vertical development and thicker ice phase precipitation zones, despite an overall decrease in the regional frequency of convection.

Figure 10 shows the variability of the global lightning source for 1998-2006 and compares it to the other NO_x emissions in GEOS-Chem. We focus on 1998-2006 because of the common availability of LIS, GFED-2, and GEOS-4 data for this period. Local scaling to the LIS/OTD climatological data (blue line in the top panel) increases the seasonal amplitude of the global lightning source relative to the unconstrained parameterization (green line), mostly because of increased lightning at northern extratropical latitudes in summer (**Table 2**). The IAV constraint (red line) produces additional variability, including in particular the summer maximum in 2004 driven by the northern subtropics.

The middle panel of **Figure 10** compares the local+IAV lightning NO_x source to the biomass burning source from the GFED2 inventory [*van der Werf et al.*, 2006] as well as other sources. The mean and interannual standard deviation of the global lightning source over these 9 years is 6.0 ± 0.5 Tg N a^{-1}, as compared to 5.5 ± 0.8 Tg N a^{-1} for the global biomass burning source. The bottom panel shows the contributions of different continents to the global lightning NO_x source. The IAV in lightning flash rates is split roughly equally between the tropics (mostly Africa) and extratropics (mostly Asia). The extratropics account for two thirds of the IAV in global lightning NO_x emissions because the NO_x yield per flash is higher there than in the tropics. In *Murray et al*. [*in prep.*], we use these emissions in a nine-year GEOS-Chem simulation to investigate the role of lightning in driving IAV of tropical tropospheric ozone and OH.

7. Conclusions

We have explored and compared different approaches for using LIS/OTD satellite observations to constrain the lightning NO_x source in global chemical transport models, with focus on enabling simulation of interannual variability (IAV) and its implications for tropospheric chemistry. A major challenge was to effectively deal with the sparseness and sampling bias of the satellite lightning data.

The standard procedure for using satellite data to constrain the lightning source in a CTM has been to start from a parameterization of lightning (based, for example, on cloud top heights or convective mass fluxes), and then apply local or regional correction (scaling) factors from the satellite data to redistribute the model lightning. Because of the sparseness of the satellite lightning data, past studies have limited themselves to climatological scaling using multiyear data [e.g., *Sauvage et al.*, 2007b; *Stajner et al.*, 2008; *Allen et al.*, 2010; *Jourdain et al.*, 2010]. We compared the local and regional climatological approaches in the GEOS-Chem CTM, using an updated LIS/OTD data set and a hierarchical clustering algorithm to optimize the selection of regions. The local scaling maximizes fidelity to the observations but the regional scaling has better statistics. We found that local and regional (coarse or fine) redistributions of lightning yield statistically indistinguishable simulations of tropospheric ozone in GEOS-Chem and that they improve significantly over the unconstrained parameterization.

We used the coherent lightning regions identified by our hierarchical clustering algorithm as the basis for constraining the IAV of lightning from the LIS data for 1998-2010 and 35ºS-35ºN, taking advantage of the better statistics afforded by scaling over coarse regions. This involved processing of the LIS data to remove the interannually varying diurnal sampling bias. The resulting time series of tropical lightning shows an interannual correlation with ENSO (R = 0.79) and no significant correlation with the solar cycle or the QBO. The resulting interannual variability of the global lightning NO_x source in GEOS-Chem (6.0 ± 0.5 Tg N a^{-1}) is similar to that of biomass burning from the GFED-2 inventory (5.5 ± 0.8 Tg N a^{-1}). About two thirds of the IAV in the global lightning NO_x source is contributed by the extratropics. In *Murray et al*. [*in prep.*], we use these interannually varying NO_x sources in GEOS-Chem to investigate the consequences for IAV of tropospheric ozone and OH.

Acknowledgments
We acknowledge useful discussions with R. V. Martin and B. Sauvage (Dalhousie), K. E. Pickering, D. Allen, L. E. Ott (UMD/UMBC/GSFC), H. Huntrieser (DLR), D. B.A. Jones (U. Toronto), and L. Jourdain (JPL). This work was supported by the NASA Atmospheric Composition Modeling and Analysis Program (ACMAP). LTM was also partly supported by the NASA Graduate Student Researchers Program and a NASA Earth and Space Science Fellowship. JAL was supported by NASA grants NNX08AJ16G and NNH09ZDA001N.

Works Cited

Allen, D., and K. Pickering (2002), Evaluation of lightning flash rate parameterizations for use in a global chemical transport model, *J Geophys Res-Atmos*, *107*, doi: 10.1029/2002JD002066.

Allen, D., K. Pickering, B. Duncan, and M. Damon (2010), Impact of lightning NO emissions on North American photochemistry as determined using the Global Modeling Initiative (GMI) model, *J Geophys Res-Atmos*, *115*, doi: 10.1029/2010JD014062.

Allen, D., K. Pickering, G. Stenchikov, A. M. Thompson, and Y. Kondo (2000), A three-dimensional total odd nitrogen (NOy) simulation during SONEX using a stretched-grid chemical transport model, *J Geophys Res-Atmos*, *105*, 3851–3876.

Auvray, M., and I. Bey (2005), Long-range transport to Europe: Seasonal variations and implications for the European ozone budget, *J Geophys Res-Atmos*, *110*, doi: 10.1029/2004JD005503.

Bey, I., D. J. Jacob, R. Yantosca, J. A. Logan, B. Field, A. Fiore, Q. Li, H. Liu, L. Mickley, and M. Schultz (2001), Global modeling of tropospheric chemistry with assimilated meteorology: Model description and evaluation, *J Geophys Res-Atmos*, *106*, 23073–23095.

Boccippio, D., W. Koshak, and R. Blakeslee (2002), Performance assessment of the Optical Transient Detector and Lightning Imaging Sensor. Part I: Predicted diurnal variability, *J Atmos Ocean Tech*, *19*(9), 1318–1332.

Boccippio, D., W. Koshak, R. Blakeslee, K. Driscoll, D. Mach, D. Buechler, W. Boeck, H. Christian, and S. Goodman (2000), The Optical Transient Detector (OTD): Instrument characteristics and cross-sensor validation, *J Atmos Ocean Tech*, *17*(4), 441–458.

Boersma, K. F., D. J. Jacob, H. J. Eskes, R. W. Pinder, J. Wang, and R. J. van der A (2008), Intercomparison of SCIAMACHY and OMI tropospheric NO2 columns: Observing the diurnal evolution of chemistry and emissions from space, *J Geophys Res-Atmos*, *113*, doi:10.1029/2007JD008816.

Chameides, W., D. Stedman, R. Dickerson, D. Rusch, and R. Cicerone (1977), NOx Production in Lightning, *J Atmos Sci*, *34*(1), 143–149.

Chatfield, R. B., J. A. Vastano, H. Singh, and G. Sachse (1996), A general model of how fire emissions and chemistry produce African/oceanic plumes (O3, CO, PAN, smoke) in TRACE A, *J Geophys Res*, *101*(D19), 24279–24,306.

Christian, H. et al. (2003), Global frequency and distribution of lightning as observed from space by the Optical Transient Detector, *J Geophys Res-Atmos*, *108*, doi: 10.1029/2002JD002347.

Christian, H., R. Blakeslee, and S. Goodman (1989), The Detection of Lightning From Geostationary Orbit, *J Geophys Res-Atmos*, *94*, 13329–13337.

Collimore, C., D. Martin, M. Hitchman, A. Huesmann, and D. Waliser (2003), On the relationship between the QBO and tropical deep convection, *J Climate*, *16*(15), 2552–2568.

Collimore, C., M. Hitchman, and D. Martin (1998), Is there a quasi-biennial oscillation in tropical deep convection?, *Geophys Res Lett*, *25*(3), 333–336.

Considine, D. B., J. A. Logan, and M. A. Olsen (2008), Evaluation of near-tropopause ozone distributions in the Global Modeling Initiative combined stratosphere/ troposphere model with ozonesonde data, *Atmos Chem Phys*, *8*(9), 2365–2385.

Cooper, O. R. et al. (2007), Evidence for a recurring eastern North America upper tropospheric ozone maximum during summer, *J Geophys Res-Atmos*, *112*, doi: 10.1029/2007JD008710.

DeCaria, A., K. Pickering, G. Stenchikov, and L. Ott (2005), Lightning-generated NOX and its impact on tropospheric ozone production: A three-dimensional modeling study of a Stratosphere-Troposphere Experiment: Radiation, Aerosols and Ozone (STERAO-A) thunderstorm, *J Geophys Res-Atmos*, *110*, doi:10.1029/2004JD005556.

Denman, K. L. et al. (2007), Couplings Between Changes in the Climate System and Biogeochemistry, in *Climate Change 2007: The Physical Science Basis*, S. Solomon, D. Qin, M. Manning, Z. Chen, M. Marquis, K. Averyt, M. Tignor, and H. Milleredited by, Cambridge University Press, Cambridge, United Kingdom and New York, NY, USA.

Duncan, B. N., and J. A. Logan (2008), Model analysis of the factors regulating the trends and variability of carbon monoxide between 1988 and 1997, *Atmos Chem Phys*, *8*(24), 7389–7403.

Duncan, B. N., J. A. Logan, I. Bey, I. A. Megretskaia, R. M. Yantosca, Novelli, P. C., N. B. Jones, and C. P. Rinsland (2007), Global budget of CO, 1988-1997: Source estimates and validation with a global model, *J Geophys Res-Atmos*, *112*, doi: 10.1029/2007JD008459.

Fishman, J., C. Watson, J. Larsen, and J. A. Logan (1990), Distribution of Tropospheric Ozone Determined From Satellite Data, *J Geophys Res-Atmos*, *95*, 3599–3617.

Fishman, J., K. Fakhruzzaman, B. Cros, and D. Nganga (1991), Identification of Widespread Pollution in the Southern-Hemisphere Deduced From Satellite Analyses, *Science*, *252*(5013), 1693–1696.

Goodman, S., D. Buechler, K. Knupp, K. Driscoll, and E. McCaul (2000), The 1997-98 El Nino event and related wintertime lightning variations in the southeastern United States, *Geophys Res Lett*, *27*(4), 541–544.

Grewe, V. (2007), Impact of climate variability on tropospheric ozone, *Sci Total Environ*, *374*(1), 167–181, doi:10.1016/j.scitotenv.2007.01.032.

Grewe, V., D. Brunner, M. Dameris, J. Grenfell, R. Hein, D. T. Shindell, and J. Staehelin (2001), Origin and variability of upper tropospheric nitrogen oxides and ozone at northern mid-latitudes, *Atmos Environ*, *35*(20), 3421–3433.

Hack, J. J. (1994), Parameterization of moist convection in the National Center for Atmospheric Research community climate model (CCM2), *J Geophys Res-Atmos*, *99*, 5551–5568.

Hamid, E., Z. Kawasaki, and R. Mardiana (2001), Impact of the 1997-98 El Nino event on lightning activity over Indonesia, *Geophys Res Lett*, *28*(1), 147–150.

Hansen, J., and S. Lebedeff (1987), Global Trends of Measured Surface Air-Temperature, *J Geophys Res-Atmos*, *92*, 13345–13372.

Hauglustaine, D., C. Granier, G. Brasseur, and G. Megie (1994), Impact of Present Aircraft Emissions of Nitrogen-Oxides on Tropospheric Ozone and Climate Forcing, *Geophys Res Lett*, *21*(18), 2031–2034.

Hudman, R. C. et al. (2007), Surface and lightning sources of nitrogen oxides over the United States: Magnitudes, chemical evolution, and outflow, *J Geophys Res-Atmos*, *112*, doi:10.1029/2006JD007912.

Huntrieser, H. et al. (2002), Airborne measurements of NOx, tracer species, and small particles during the European lightning nitrogen oxides experiment, *J Geophys Res-Atmos*, *107*, doi:10.1029/2000JD000209.

Huntrieser, H., H. Schlager, A. Roiger, M. Lichtenstern, U. Schumann, C. Kurz, D. Brunner, C. Schwierz, A. Richter, and A. Stohl (2007), Lightning-produced NOx over Brazil during TROCCINOX: airborne measurements in tropical and subtropical thunderstorms and the importance of mesoscale convective systems, *Atmos Chem Phys*, *7*(11), 2987–3013.

Huntrieser, H., U. Schumann, H. Schlager, H. Hoeller, A. Giez, H. D. Betz, D. Brunner, C. Forster, O. J. Pinto, and R. Calheiros (2008), Lightning activity in Brazilian thunderstorms during TROCCINOX: implications for NOx production, *Atmos Chem Phys*, *8*(4), 921–953.

Jacob, D. J. et al. (1996), Origin of ozone and NOx in the tropical troposphere: A photochemical analysis of aircraft observations over the South Atlantic basin, *J Geophys Res-Atmos*, *101*, 24235–24250.

Jacobson, M. Z., and D. G. Streets (2009), Influence of future anthropogenic emissions on climate, natural emissions, and air quality, *J Geophys Res-Atmos*, *114*, doi: 10.1029/2008JD011476.

Jaeglé, L., D. J. Jacob, W. Brune, and P. Wennberg (2001), Chemistry of HOx radicals in the upper troposphere, *Atmos Environ*, *35*(3), 469–489.

Johnson, S. (1967), Hierarchical Clustering Schemes, *Psychometrika*, *32*(3), 241–254.

Jourdain, L., S. S. Kulawik, H. M. Worden, K. E. Pickering, J. Worden, and A. M. Thompson (2010), Lightning NOx emissions over the USA constrained by TES ozone observations and the GEOS-Chem model, *Atmos Chem Phys*, *10*(1), 107–119.

Koshak, W. J., M. Stewart, H. Christian, J. Bergstrom, J. Hall, and R. Solakiewicz (2000), Laboratory calibration of the optical transient detector and the lightning imaging sensor, *J Atmos Ocean Tech*, *17*(7), 905–915.

Koshak, W. J., Peterson, H. S., Khan, M., Biazar, A. P., Wang, L., (2012). The NASA
Lightning Nitrogen Oxides Model (LNOM): Application to Air Quality
Modeling, *Atmos. Res.*, *in review*.

Krishnamurti, T., H. Fuelberg, M. Sinha, D. Oosterhof, E. Bensman, and V. Kumar (1993), The Meteorological Environment of the Tropospheric Ozone Maximum Over the Tropical South-Atlantic Ocean, *J Geophys Res-Atmos*, *98*, 10621–10641.

Kuhns, H., M. Green, and V. Etyemezian (2003), Big Bend Regional Aerosol and Visibility Observational (BRAVO) Study Emissions Inventory,

Labrador, L., R. von Kuhlmann, and M. Lawrence (2004), Strong sensitivity of the global mean OH concentration and the tropospheric oxidizing efficiency to the source of NOx from lightning, *Geophys Res Lett*, *31*(6), doi:10.1029/2003GL019229.

Levelt, P., G. Van den Oord, M. Dobber, A. Malkki, H. Visser, J. de Vries, P. Stammes, J. Lundell, and H. Saari (2006), The Ozone Monitoring Instrument, *IEEE T Geosci Remote*, *44*(5), 1093–1101, doi:10.1109/TGRS.2006.872333.

Logan, J. A., I. Megretskaia, R. Nassar, L. T. Murray, L. Zhang, K. W. Bowman, H. M. Worden, and M. Luo (2008), Effects of the 2006 El Nino on tropospheric composition as revealed by data from the Tropospheric Emission Spectrometer (TES), *Geophys Res Lett*, *35*(3), doi:10.1029/2007GL031698.

Logan, J. A., M. Prather, S. C. Wofsy, and M. McElroy (1981), Tropospheric Chemistry - a Global Perspective, *J Geophys Res-Oc Atm*, *86*, 7210–7254.

Mach, D. M., H. J. Christian, R. J. Blakeslee, D. J. Boccippio, S. J. Goodman, and W. L. Boeck (2007), Performance assessment of the Optical Transient Detector and Lightning Imaging Sensor, *J Geophys Res-Atmos*, *112*, doi:10.1029/2006JD007787.

Marshall, T., and M. Stolzenburg (2001), Voltages inside and just above thunderstorms, *J Geophys Res-Atmos*, *106*, 4757–4768.

Martin, R. et al. (2002), Interpretation of TOMS observations of tropical tropospheric ozone with a global model and in situ observations, *J Geophys Res-Atmos*, *107*, doi: 10.1029/2001JD001480.

Martin, R. V., B. Sauvage, I. Folkins, C. E. Sioris, C. Boone, P. Bernath, and J. R. Ziemke (2007), Space-based constraints on the production of nitric oxide by lightning, *J Geophys Res-Atmos*, *112*, doi:10.1029/2006JD007831.

Martin, R. V., C. E. Sioris, K. Chance, T. B. Ryerson, T. H. Bertram, P. J. Wooldridge, R. C. Cohen, J. A. Neuman, A. Swanson, and F. M. Flocke (2006), Evaluation of space-based constraints on global nitrogen oxide emissions with regional aircraft measurements over and downwind of eastern North America, *J Geophys Res-Atmos*, *111*, doi:10.1029/2005JD006680.

Meijer, E., P. van Velthoven, D. Brunner, H. Huntrieser, and H. Kelder (2001), Improvement and evaluation of the parameterisation of nitrogen oxide production by lightning, *Phys Chem Earth Pt C*, *26*(8), 577–583.

Montzka, S. A., M. Krol, E. Dlugokencky, B. Hall, P. Joeckel, and J. Lelieveld (2011), Small Interannual Variability of Global Atmospheric Hydroxyl, *Science*, *331*(6013), 67–69, doi:10.1126/science.1197640.

Murray, L. T., J. A. Logan, and D. J. Jacob, The role of lightning in driving interannual variability in tropical tropospheric ozone and OH, *in preparation*.

Olivier, J. G. (2001), *Global emissions sources and sinks*, The Climate System, A. A. Balkema Publishers/Swets & Zeitlinger Publishers, Lisse, Netherlands.

Ott, L. E., K. E. Pickering, G. L. Stenchikov, D. J. Allen, A. J. DeCaria, B. Ridley, R.-F. Lin, S. Lang, and W.-K. Tao (2010), Production of lightning NOx and its vertical

distribution calculated from three-dimensional cloud-scale chemical transport model simulations, *J Geophys Res-Atmos*, *115*, doi:10.1029/2009JD011880.

Ott, L. E., K. E. Pickering, G. L. Stenchikov, H. Huntrieser, and U. Schumann (2007), Effects of lightning NOx production during the 21 July European Lightning Nitrogen Oxides Project storm studied with a three-dimensional cloud-scale chemical transport model, *J Geophys Res-Atmos*, *112*, doi:10.1029/2006JD007365.

Petersen, W., H. Christian, and S. Rutledge (2005), TRMM observations of the global relationship between ice water content and lightning, *Geophys Res Lett*, *32*(14), doi: 10.1029/2005GL023236.

Pickering, K., A. M. Thompson, R. Dickerson, W. Luke, D. Mcnamara, J. Greenberg, and P. Zimmerman (1990), Model-Calculations of Tropospheric Ozone Production Potential Following Observed Convective Events, *J Geophys Res-Atmos*, *95*, 14049–14062.

Pickering, K., A. M. Thompson, W. Tao, and T. Kucsera (1993), Upper Tropospheric Ozone Production Following Mesoscale Convection During STEP/EMEX, *J Geophys Res-Atmos*, *98*, 8737–8749.

Pickering, K., Y. Wang, W. Tao, C. Price, and J. Muller (1998), Vertical distributions of lightning NOx for use in regional and global chemical transport models, *J Geophys Res-Atmos*, *103*, 31203–31216.

Price, C., and D. Rind (1992), A Simple Lightning Parameterization for Calculating Global Lightning Distributions, *J Geophys Res-Atmos*, *97*, 9919–9933.

Price, C., and D. Rind (1993), What Determines the Cloud-to-Ground Lightning Fraction in Thunderstorms, *Geophys Res Lett*, *20*(6), 463–466.

Price, C., and D. Rind (1994), Modeling Global Lightning Distributions in a General-Circulation Model, *Mon Weather Rev*, *122*(8), 1930–1939.

Price, C., J. Penner, and M. Prather (1997), NOx from lightning .1. Global distribution based on lightning physics, *J Geophys Res-Atmos*, *102*, 5929–5941.

Prinn, R. et al. (2005), Evidence for variability of atmospheric hydroxyl radicals over the past quarter century, *Geophys Res Lett*, *32*(7), doi:10.1029/2004GL022228.

Rakov, V. A., and M. A. Uman (2003), *Lightning Physics and Effects*, Cambridge University Press, Cambridge, United Kingdom.

Sauvage, B., R. V. Martin, A. van Donkelaar, and J. R. Ziemke (2007a), Quantification of the factors controlling tropical tropospheric ozone and the South Atlantic maximum, *J Geophys Res-Atmos*, *112*, doi:10.1029/2006JD008008.

Sauvage, B., R. V. Martin, A. van Donkelaar, X. Liu, K. Chance, L. Jaeglé, P. I. Palmer, S. Wu, and T. M. Fu (2007b), Remote sensed and in situ constraints on processes affecting tropical tropospheric ozone, *Atmos Chem Phys*, *7*, 815–838.

Sauvage, B., V. Thouret, A. M. Thompson, J. Witte, J. Cammas, P. Nedelec, and G. Athier (2006), Enhanced view of the "tropical Atlantic ozone paradox" and "zonal wave one“” from the in situ MOZAIC and SHADOZ data, *J Geophys Res-Atmos*, *111*, doi: 10.1029/2005JD006241.

Schumann, U., and H. Huntrieser (2007), The global lightning-induced nitrogen oxides source, *Atmos Chem Phys*, *7*(14), 3823–3907.

Shiotani, M. (1992), Annual, Quasi-Biennial, and El Niño-Southern Oscillation (ENSO) Time-Scale Variations in Equatorial Total Ozone, *J Geophys Res-Atmos*, *97*, 7625–7633.

Stajner, I. et al. (2008), Assimilated ozone from EOS-Aura: Evaluation of the tropopause region and tropospheric columns, *J Geophys Res-Atmos*, *113*, doi: 10.1029/2007JD008863.

Streets, D. et al. (2003), An inventory of gaseous and primary aerosol emissions in Asia in the year 2000, *J Geophys Res-Atmos*, *108*, doi:10.1029/2002JD003093.

Streets, D. G., Q. Zhang, L. Wang, K. He, J. Hao, Y. Wu, Y. Tang, and G. R. Carmichael (2006), Revisiting China's CO emissions after the Transport and Chemical Evolution over the Pacific (TRACE-P) mission: Synthesis of inventories, atmospheric modeling, and observations, *J Geophys Res-Atmos*, *111*, doi:10.1029/2006JD007118.

Thompson, A. M. et al. (2003a), Southern Hemisphere Additional Ozonesondes (SHADOZ) 1998-2000 tropical ozone climatology - 1. Comparison with Total Ozone Mapping Spectrometer (TOMS) and ground-based measurements, *J Geophys Res-Atmos*, *108*, doi:10.1029/2001JD000967.

Thompson, A. M. et al. (2003b), Southern Hemisphere Additional Ozonesondes (SHADOZ) 1998-2000 tropical ozone climatology - 2. Tropospheric variability and the zonal wave-one, *J Geophys Res-Atmos*, *108*, doi:10.1029/2002JD002241.

Thompson, A. M., and R. Hudson (1999), Tropical tropospheric ozone (TTO) maps from Nimbus 7 and Earth Probe TOMS by the modified-residual method: Evaluation with sondes, ENSO signals, and trends from Atlantic regional time series, in *Journal of Geophysical Research-Atmospheres*, vol. 104, pp. 26961–26975.

Thompson, A. M., B. Doddridge, J. Witte, R. Hudson, W. Luke, J. Johnston, B. Johnston, S. Oltmans, and R. Weller (2000), A tropical Atlantic paradox: Shipboard and satellite views of a tropospheric ozone maximum and wave-one in January-February 1999., *Geophys Res Lett*, *27*(20), 3317–3320.

Tost, H., P. J. Joeckel, and J. Lelieveld (2007), Lightning and convection parameterisations - uncertainties in global modelling, *Atmos Chem Phys*, *7*(17), 4553–4568.

van der Werf, G. R., J. T. Randerson, L. Giglio, G. J. Collatz, P. S. Kasibhatla, and A. F. J. Arellano (2006), Interannual variability in global biomass burning emissions from 1997 to 2004, *Atmos Chem Phys*, *6*, 3423–3441.

Wang, Y., D. J. Jacob, and J. A. Logan (1998), Global simulation of tropospheric O3-NOx-hydrocarbon chemistry 1. Model formulation, *J Geophys Res-Atmos*, *103*, 10713–10725.

Waters, J. et al. (2006), The Earth Observing System Microwave Limb Sounder (EOS MLS) on the Aura satellite, *IEEE T Geosci Remote*, *44*(5), 1075–1092, doi:10.1109/TGRS.2006.873771.

Williams, E. (1985), Large-Scale Charge Separation in Thunderclouds, *J Geophys Res-Atmos*, *90*, 6013–6025.

Williams, E. (1992), The Schumann Resonance - a Global Tropical Thermometer, *Science*, *256*(5060), 1184–1187.

Wu, S., L. J. Mickley, D. J. Jacob, J. A. Logan, R. M. Yantosca, and D. Rind (2007), Why are there large differences between models in global budgets of tropospheric ozone?, *J Geophys Res-Atmos*, *112*, doi:10.1029/2006JD007801.

Yevich, R., and J. A. Logan (2003), An assessment of biofuel use and burning of agricultural waste in the developing world, *Global Biogeochem Cy*, *17*(4), doi: 10.1029/2002GB001952.

Yienger, J., and H. Levy (1995), Empirical-Model of Global Soil-Biogenic NOx Emissions, *J Geophys Res-Atmos*, *100*, 11447–11464.

Yoshida, S., T. Morimoto, T. Ushio, and Z. Kawasaki (2007), ENSO and convective activities in Southeast Asia and western Pacific, *Geophys Res Lett*, *34*(21), doi: 10.1029/2007GL030758.

Zhang, G., and N. McFarlane (1995), Sensitivity of Climate Simulations to the Parameterization of Cumulus Convection in the Canadian Climate Center General-Circulation Model, *Atmos Ocean*, *33*(3), 407–446.

Ziemke, J. R., and S. Chandra (1999), Seasonal and interannual variabilities in tropical tropospheric ozone, *J Geophys Res-Atmos*, *104*, 21425–21442.

Ziemke, J. R., S. Chandra, B. N. Duncan, L. Froidevaux, P. K. Bhartia, P. F. Levelt, and J. W. Waters (2006), Tropospheric ozone determined from aura OMI and MLS: Evaluation of measurements and comparison with the Global Modeling Initiative's Chemical Transport Model, *J Geophys Res-Atmos*, *111*, doi:10.1029/2006JD007089.

LaTeX Equations

```
\alpha = \beta \left. \iint\limits_D F_{o}(\mathrm{\bf{x}},t)\;\mathrm{d\bf{x}}\;
\mathrm{d}t \middle/ \iint\limits_D F_{p}(\mathrm{\bf{x}},t)\;\mathrm{d\bf{x}}\;
\mathrm{d}t \right.
```

Figures

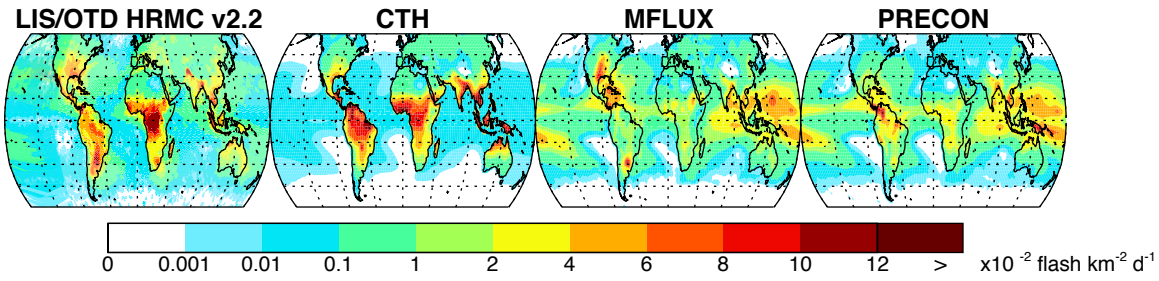

Figure 1. Mean lightning densities (flashes km^{-2} d^{-1}) for May 1995 to December 2005. LIS/OTD satellite data from the High Resolution Monthly Climatology (HRMC) v2.2 are compared to unconstrained GEOS-Chem model distributions from parameterizations based on cloud top height (CTH) [*Price and Rind*, 1992; 1993; 1994], upward mass flux (MFLUX) [*Allen et al*., 2000], and convective precipitation (PRECON) [*Allen and Pickering*, 2002].

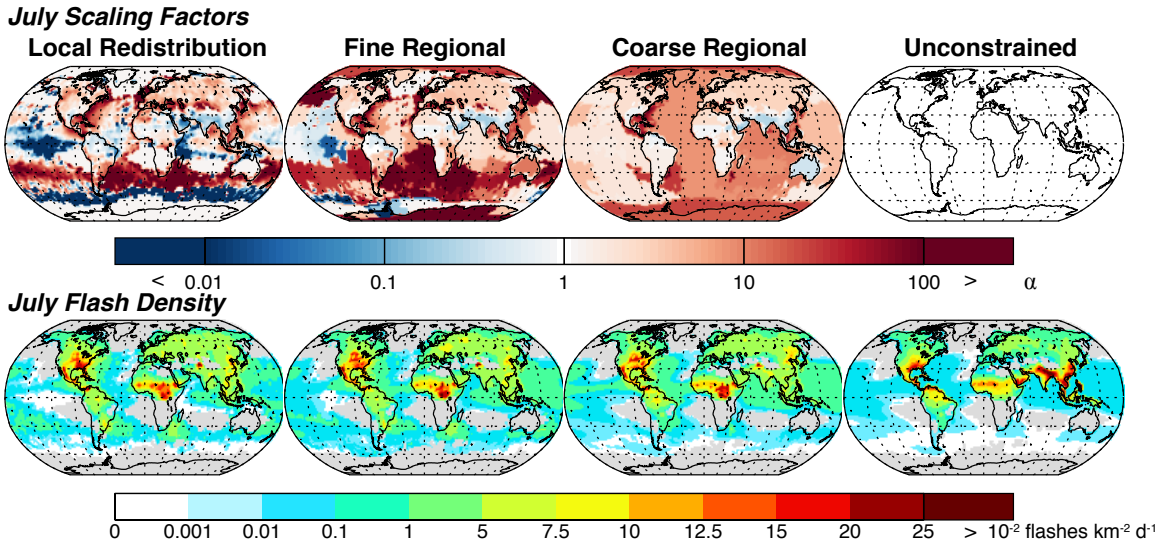

Figure 2. Spatial redistribution of lightning flash densities in GEOS-Chem to match the LIS/OTD HRMC data for July. Results from the local, fine regional, and coarse regional redistributions are compared and the unconstrained distribution is also shown. The top panels show the log of the scaling factors α computed from equation (1). The bottom panels show the corresponding July lightning flash distributions averaged over 1995-2005. The bottom left panel (local adjustment) essentially corresponds to the July LIS/OTD climatology. Gray regions have no lightning in GEOS-Chem. Statistics for the different redistributions are given in Table 2.

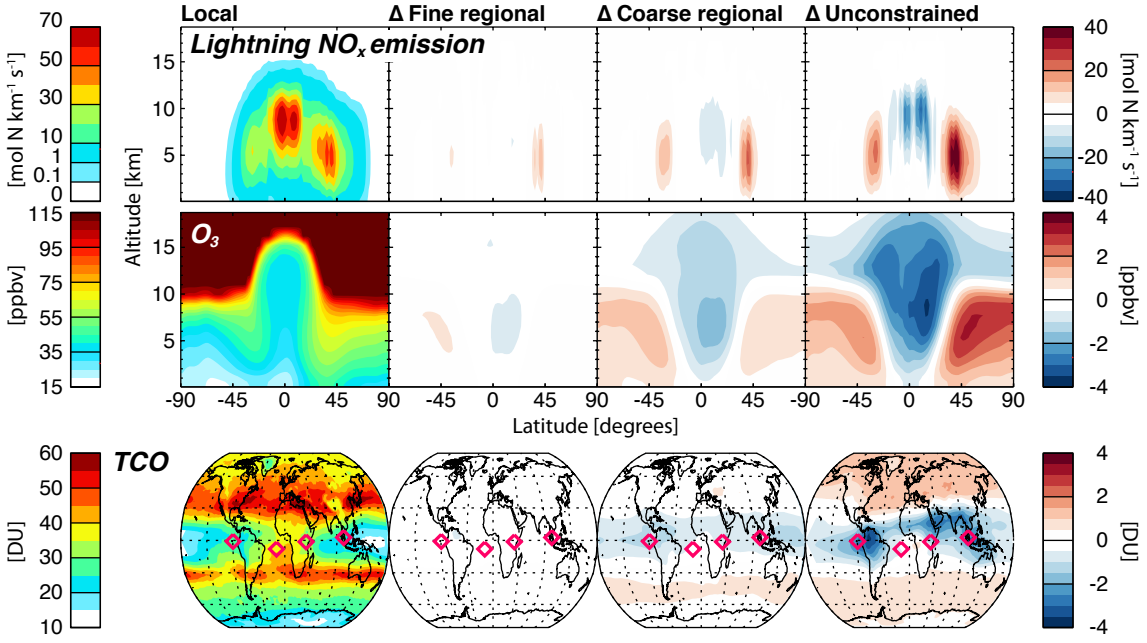

Figure 3. Effect of different lightning redistributions on lightning NO_x emissions and tropospheric ozone mixing ratios in GEOS-Chem. The left panels show annual mean results from a simulation for 2004-2005 with local redistribution based on the LIS/OTD HRMC satellite climatology: zonal mean lightning NO_x emissions (top), zonal mean ozone profiles (middle), and tropospheric column of ozone (TCO). The other panels show the differences (Δ) relative to that simulation when the regional redistribution is used (fine or coarse) or when no redistribution is applied (unconstrained). The diamonds show the location of stations used in Figure 4.

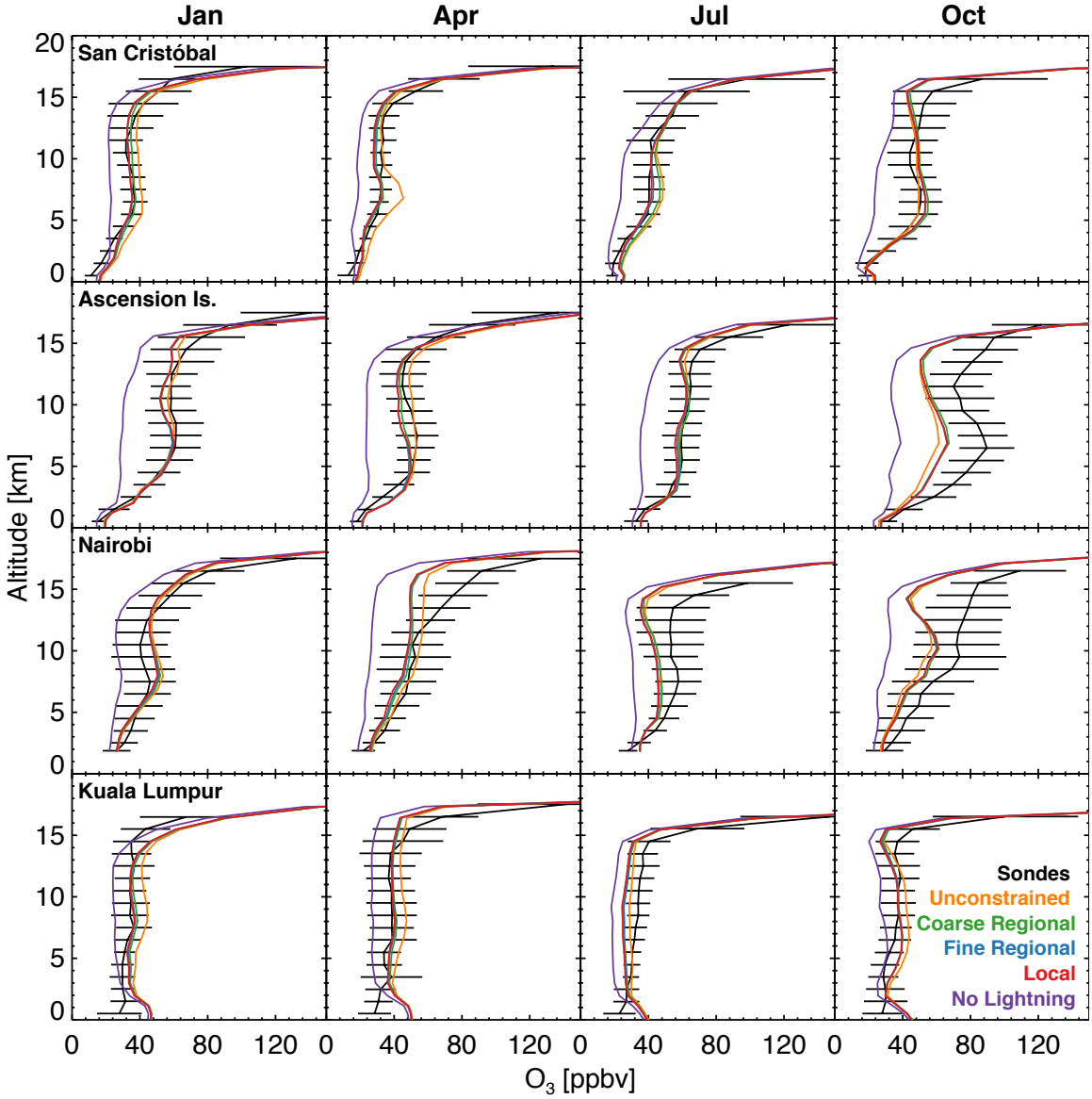

Figure 4. Monthly mean vertical profiles of ozone (in ppbv) for four tropical stations of the SHADOZ ozonesonde network [*Thompson et al*., 2003a]: San Cristóbal, Ecuador (0.9ºS, 89.6ºW), Ascension Island (8.0ºS, 14.4ºW), Nairobi, Kenya (1.3ºS, 36.8ºE), and Kuala Lumpur, Malaysia (2.7ºN, 101.7ºE). Plotted in black are observed mean profiles for 1998-2010 with bars indicating standard deviations of the individual profiles for 1 km vertical bins. The colored lines represent the mean daily ozone profiles for 2004-2005 simulated by GEOS-Chem using the different lightning redistributions. Also shown is a simulation without lightning NO_x (purple).

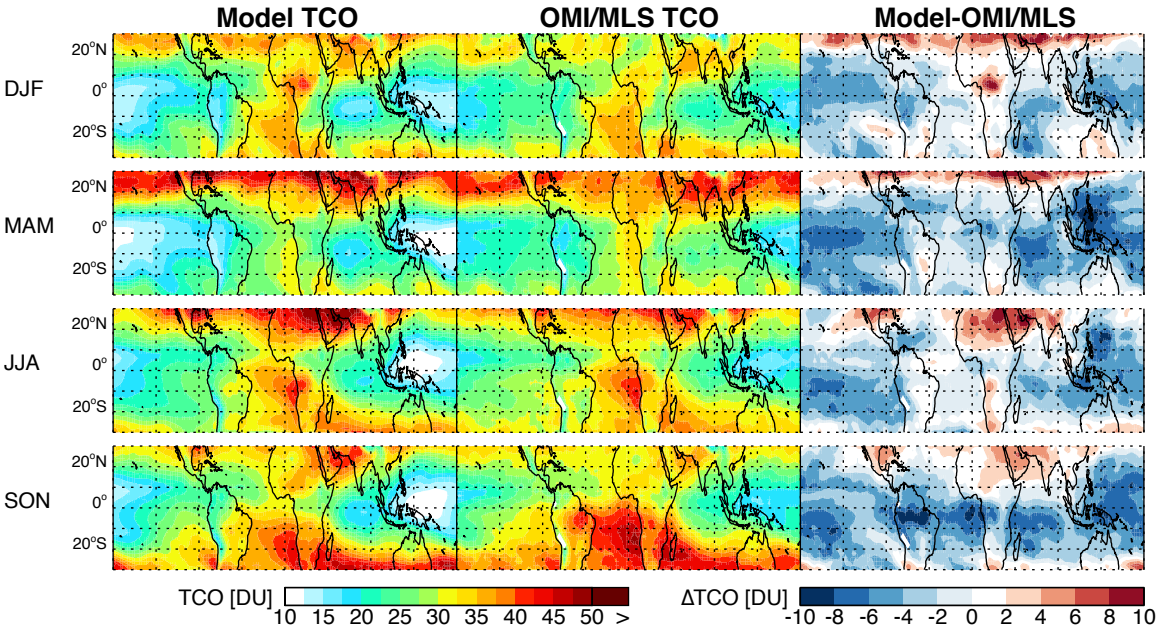

Figure 5. Seasonal mean tropospheric column ozone (TCO) for December 2004 to November 2005. Model results using the local lightning redistribution are compared to OMI/MLS observations [*Ziemke et al*., 2006] available from ftp://jwocky.gsfc.nasa.gov/pub/ccd/data_monthly. The right panels show the differences between the two.

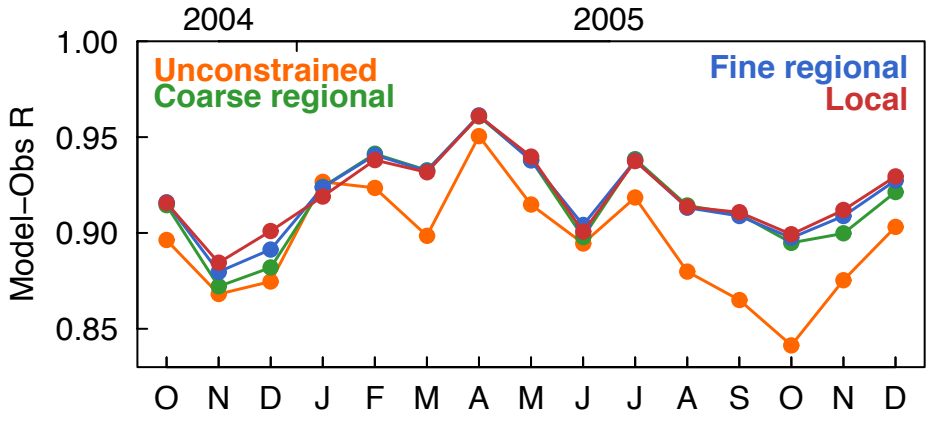

Figure 6. Spatial correlation coefficient R for GEOS-Chem versus OMI/MLS monthly mean tropospheric column ozone (TCO) on the 2ºx2.5º grid of GEOS-Chem and for 23ºS-23ºN. Values are for October 2004 to December 2005.

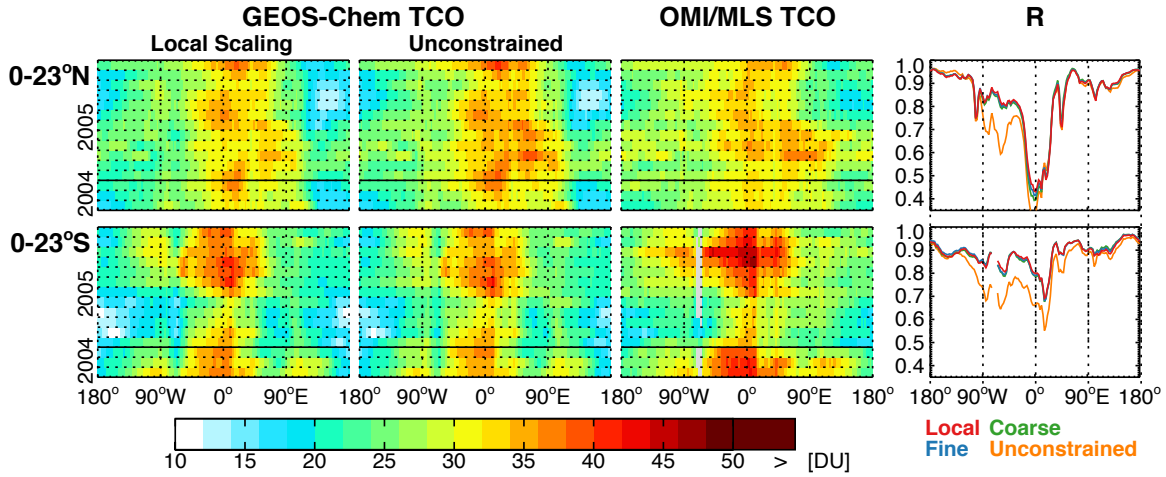

Figure 7. Tropospheric column ozone (TCO) in the 0-23ºN and 0-23ºS bands as a function of longitude and time for October 2004 to December 2005. Observations from OMI/MLS are compared to GEOS-Chem simulations with the unconstrained lightning parameterization and with local lightning redistribution based on the LIS/OTD data. The right panels show the correlation coefficients of simulated versus observed values for specified longitudes and months (n = 12 latitudes per hemisphere on the 2ºx2.5º model grid x 15 months), for the simulations with unconstrained lightning and with different lightning redistributions.

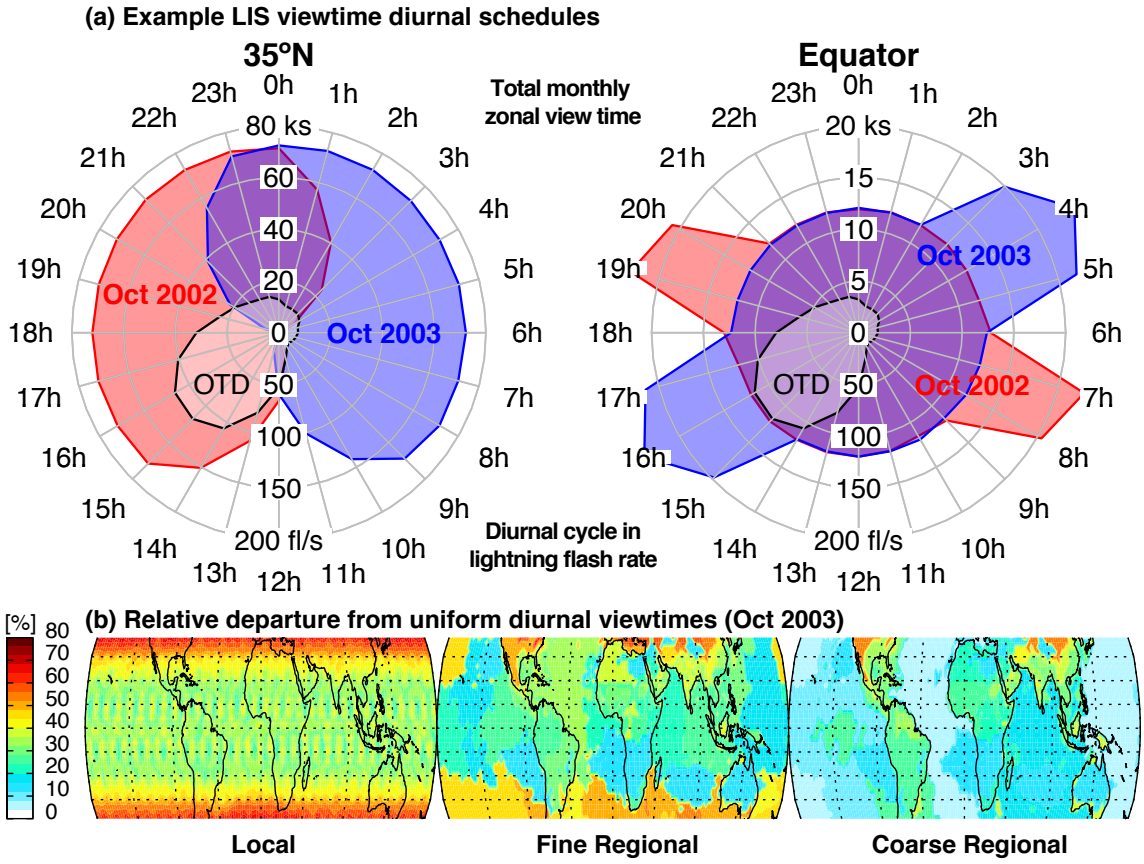

Figure 8. Diurnal distribution of LIS satellite observations for October 2002 and 2003. The top panel shows rose plots of the total LIS viewing times (kiloseconds or ks) at different local times of day for October 2002 (red and purple) and October 2003 (blue and purple) aggregated zonally over 2º latitudinal bands at 35ºN and the Equator. Note the difference in scales for 35ºN and the Equator, as 35ºN is observed ten times more frequently because of the inclined satellite orbit. Also shown in the same rose plots is the climatological global frequency of lightning (flashes per second or fl/s) as a function of local time of day measured by the OTD satellite instrument in sun-asynchronous near-polar orbit. The bottom panels display the LIS diurnal sampling bias for October 2003 as the mean relative departure of hourly observation frequencies from 24-h uniform sampling. A region with uniform sampling would have a relative departure of 0%, while a region with twice as frequent sampling in the daytime than at night would show a relative departure of 33%.

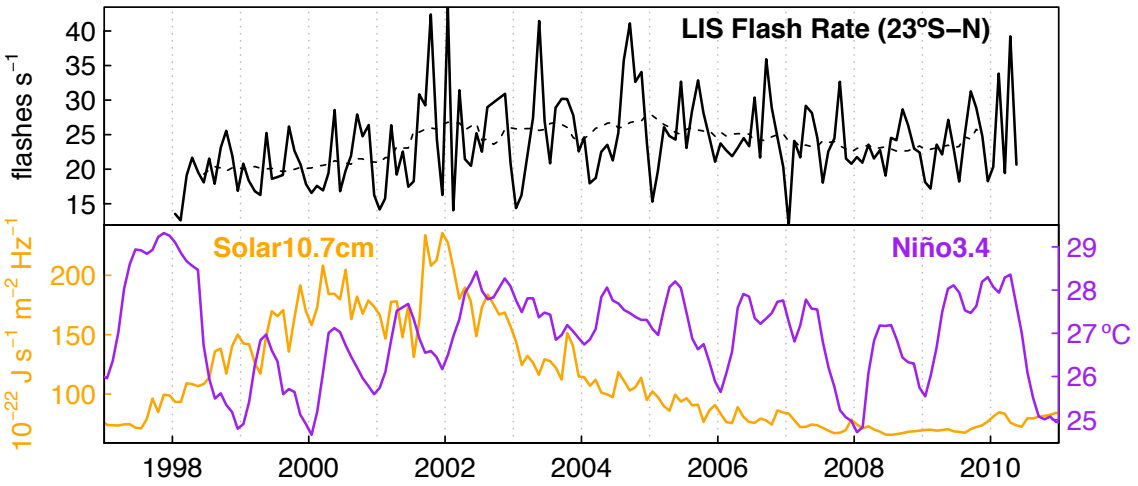

Figure 9. 1998-2010 interannual variability (IAV) of tropical lightning and climatological indices for 23ºS-23ºN. Top panel: time series of the monthly mean tropical flash rate determined from the LIS Science Data v4.1 product as described in the text. The dashed line is the 12- month running mean. Bottom panel: climatological indices available from NOAA ESRL (http://www.esrl.noaa.gov/psd/data/climateindices/), including the monthly mean Solar Flux (10.7cm; orange) provided as a service by the National Research Council of Canada, and the El Niño Region 3.4 Index (Niño3.4; purple).

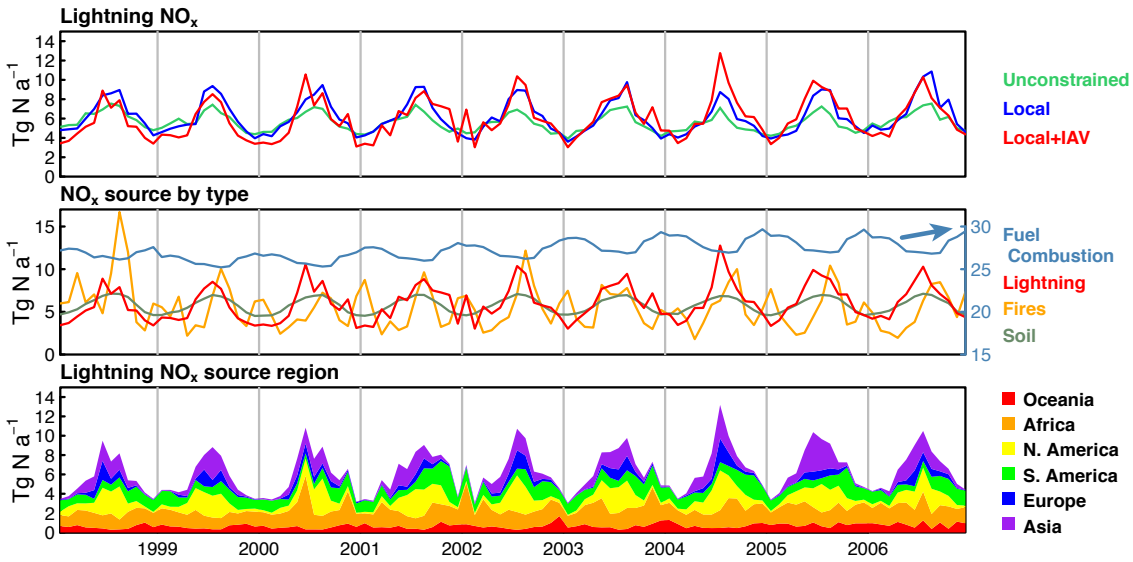

Figure 10. Global monthly NO_x emissions, 1998-2006. Top panel: lightning emissions computed from the unconstrained parameterization, the parameterization with local climatological scaling from the LIS/OTD data, and the simulation with local scaling and coarse regional interannual variability (IAV) from the LIS data. Middle panel: NO_x emissions by source type where lightning is from the local scaling with IAV; note different scale on the right for the anthropogenic NO_x source (fossil fuel and biofuel). Bottom panel: cumulative lightning NO_x emissions (including local scaling and IAV) by continent. The time series of lightning NO_x emissions including local scaling and IAV is reproduced in all three panels.

Tables

Table 1. Sources of tropospheric NO_x in GEOS-Chem[a]

Source	**Tg N a^{-1}**
Fossil fuel and biofuel combustion[b]	27.8
Lightning	5.8
Soil microbial activity[c]	5.6
Open fires	5.3
Transport from stratosphere[d]	0.8
Total	45.3

[a.] Annual means for 2004-2005
[b.] Including 0.5 Tg N a^{-1} from aircraft emissions at cruise altitude
[c.] Including 0.7 Tg N a^{-1} from fertilizer application
[d.] NO_x tracked across the monthly mean tropopause.

Table 2. Global lightning redistribution statistics for matching GEOS-Chem to LIS/OTD constraints[a]

Redistribution	Number of regions[b]	Range of scaling factors[c]	R	Lightning distribution[d]		Global lightning NO_x source[e], Tg N a^{-1}	Monthly LIS overpasses per region[f]
				tropics	northern extratropics		
Local	13,104	10^{-11} - 10^{+4}	>0.99	65%	23%	6.1	67
Fine Regional	137	10^{-10} - 10^{+3}	0.93	68%	22%	6.0	406
Coarse Regional	37	10^{-5} - 10^{+2}	0.89	74%	20%	6.0	1044
Unconstrained[g]	1	1	0.66	84%	13%	5.6	-

[a] The redistributions constrain the lightning flash statistics in the GEOS-Chem CTM to match the monthly observed LIS/OTD HRMC v2.2 climatology over local or regional scaling domains *D*. The Pearson correlation coefficients R measure the fit between the resulting GEOS-Chem and LIS/OTD long-term monthly mean climatologies on the 2ºx2.5º grid of the model (n = 144 longitudes x 91 latitudes x 12 months).

[b] The number of regions can vary slightly from month to month with regional scaling and the values given here are annual means.

[c] Global range of scaling factors α computed from equation (1).

[d] Fraction of global simulated flashes in the tropics (23ºS-23ºN) and northern extratropics (23º-90ºN).

[e] Redistribution affects the global lightning NO_x source because of the difference in the NO_x yield per flash between the tropics and the extratropics (section 4.3).

[f] Mean number of LIS orbital overpasses per region in the month of October, calculated for data from 1998 to 2006.

[g] Original CTH parameterization of lightning in GEOS-Chem with no redistribution (section 4.1).